

Novel $\text{In}_{0.425}\text{Al}_{0.575}\text{As}/\text{In}_x\text{Ga}_{1-x}\text{As}$ Metamorphic δ -HEMT's on GaAs Substrate with Various Channel Designs

Wei-Chou Hsu¹, Ching-Sung Lee², Yeong-Jia Chen¹, Jun-Chin Huang¹, and Chang-Luen Wu³

¹Institute of Microelectronics, Department of Electrical Engineering, National Cheng-Kung University
1, University Road, Tainan, Taiwan 70101, R.O.C.

²Department of Electronic Engineering, Feng Chia University
100, Wenhwa Road, Taichung, Taiwan 40724, R.O.C.

Tel: +886-4-24517250 #4953, Fax: +886-4-24721858 E-mail : cslee@fcu.edu.tw

³Transcom, Inc., 90, Da-Shun 7th Road, Tainan Science-Based Industrial Park
Hsin-Shi, Tainan County, Taiwan 744, R.O.C.

1. Introduction

Novel $\text{In}_{0.425}\text{Al}_{0.575}\text{As}/\text{In}_x\text{Ga}_{1-x}\text{As}$ metamorphic high electron mobility transistors, grown on GaAs substrate [1-3] by MBE system, either with a V-shaped symmetrically-graded channel (SGC-MHEMT) or with a pseudomorphic $\text{In}_{0.65}\text{Ga}_{0.35}\text{As}$ channel MHEMT (PC-MHEMT) have been successfully investigated in this work. Device characteristics, including the extrinsic transconductance, current driving capability, device linearity, pinch-off property, gate-voltage swing, breakdown performance, unity-gain cutoff frequency, max. oscillation frequency, output power, and power gain, have been comprehensively compared and discussed with respect to their respective channel designs.

2. Layer Structure and Device Fabrication

Layer structure of the proposed δ -doped $\text{In}_{0.425}\text{Al}_{0.575}\text{As}/\text{In}_x\text{Ga}_{1-x}\text{As}$ SGC-MHEMT, grown on (100) S.I. GaAs substrate, consists of a 0.5 μm $\text{In}_x\text{Al}_{1-x}\text{As}$ graded (x : 0 to 0.45 upwardly) metamorphic buffer layer, followed by a 150 nm thick undoped $\text{In}_{0.425}\text{Al}_{0.575}\text{As}$ barrier layer, a 20 nm undoped V-shaped symmetrically-graded $\text{In}_x\text{Ga}_{1-x}\text{As}$ channel ($x = 0.5 \rightarrow 0.65 \rightarrow 0.5$), a 5 nm undoped $\text{In}_{0.425}\text{Al}_{0.575}\text{As}$ spacer, a Si δ -doped layer ($4 \times 10^{12} \text{ cm}^{-2}$), a 25 nm undoped $\text{In}_{0.425}\text{Al}_{0.575}\text{As}$ Schottky layer, a 2.5 nm undoped InP etch-stopper and finally a 20 nm Si-doped ($1 \times 10^{19} \text{ cm}^{-3}$) $\text{In}_{0.5}\text{Ga}_{0.5}\text{As}$ capper. A 20 nm undoped $\text{In}_{0.65}\text{Ga}_{0.35}\text{As}$ pseudomorphic layer was employed, instead, as channel for the PC-MHEMT. The inverse step-graded buffer design was applied to both structures to provide good relaxation from lattice strain within the active layers [4]. Standard photolithography, lift-off and rapid thermal annealing (RTA) techniques were employed for device fabrication. AuGe/Ni/Au alloys were used for source and drain ohmic contacts. Au was deposited on the undoped InAlAs Schottky layer as the gate electrode. The gate dimensions were $0.65 \times 200 \mu\text{m}^2$.

3. Experimental Results and Discussions

As in indicated in Fig. 1, both devices demonstrates superior pinch-off characteristics due to the use of wide-gap $\text{In}_{0.425}\text{Al}_{0.575}\text{As}$ barrier and high resistivity metamorphic buffer to greatly suppress the substrate leakages.

Since lower impact threshold field accompanies with narrower energy-gap as increasing the In composition in $\text{In}_x\text{Ga}_{1-x}\text{As}$ channel, improved impact ionization effects by using the V-shaped symmetrically-graded channel in SGC-MHEMT (than PC-MHEMT) can be achieved, resulting in lower output conductance, g_d , of 11 (13) mS/mm, and higher device gain, $A_v = g_m/g_d$, of 24.6 (23.2). On the other hand, better carrier confinement was obtained due to higher conduction band discontinuities by using the In-rich $\text{In}_{0.65}\text{Ga}_{0.35}\text{As}$ channel in PC-MHEMT (than SGC-MHEMT), leading to the improved max. extrinsic transconductance, $g_{m, \text{max}}$, of 315 (271) mS/mm and saturation current density, I_{DSS} , 548 (469) mA/mm, as shown in Fig. 2. Nevertheless, the gate-voltage swing (GVS), defined at the drop of 10% from $g_{m, \text{max}}$, was improved by 30% in SGC-MHEMT, due to the V-shaped linearly-graded channel design. SGC-MHEMT has also demonstrated better gate leakages and forward turn-on characteristics than PC-MHEMT, as indicated in Fig. 3 and its inset, since higher effective energy-gap of $\text{In}_x\text{Ga}_{1-x}\text{As}$ channel was designed in SGC-MHEMT. Figure 4 and 5 also characterizes the off-state breakdown and on-state gate leakage performances, respectively, by using the drain-current injection technique [5] and by identifying from the observed "bell-shaped" behaviors. Figures 6 and 7 compare the cut-off frequency, f_T , of 55.4 (42.8) GHz, the max. oscillation frequency, f_{max} , of 77.5 (50.8) GHz, the saturated output power, P_{out} , of 12.5 (14.7) dBm, and the small-signal power gain, G_S , of 16.5 (19.2) dB for PC-MHEMT (SGC-MHEMT), respectively.

4. Conclusions

Large scale millimeter-wave integrated circuits (MMIC's) can be realized by employing a metamorphic $\text{In}_x\text{Al}_{1-x}\text{As}$ graded buffer on GaAs substrates. With the distinguished channel designs, the proposed PC-MHEMT and SGC-MHEMT are promising for high-frequency circuits and high-power with improved linearity circuits applications, respectively.

Acknowledgements - This work was supported by the National Science Council, R.O.C., under contract numbers of NSC 93-2215-E-006-007 and NSC 93-2215-E-035-005.

References

- [1] K. Ouchi, T. Mishima, M. Kudo and H. Ohta, *Jpn. J. Appl. Phys.* **41** (2002) 1004.
- [2] S. Bollaert, Y. Cordier, M. Zaknoute, H. Happy, S. Lpilliet, A. Cappy, *Proc. Indium Phosphide and Related Materials* (2001) 192.
- [3] W. C. Hsu, Y. J. Chen, C. S. Lee, T. B. Wang, Y. S. Lin, and C. L. Wu, *IEEE Electron Device Lett.* **26** (2005) 59.
- [4] Y. Cordier, S. Bollaert, J. Dipersio, D. Ferre, S. Trudel, Y. Druelle and A. Cappy, *Appl. Surf. Sci.* **123/124** (1998) 734.
- [5] S. R. Bahl, J. A. del Alamo, J. Dickmann, and S. Schildberg, *IEEE Trans. Electron. Devices* **42** (1995) 15.

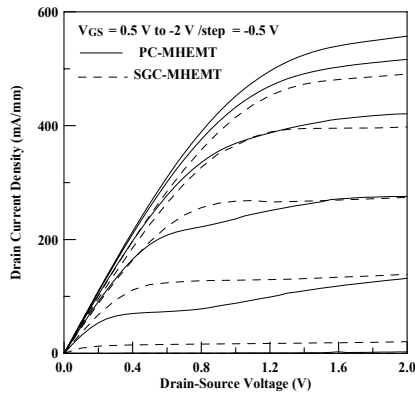


Fig. 1 Room-temperature I-V characteristics for PC-MHEMT and SGC-MHEMT, respectively.

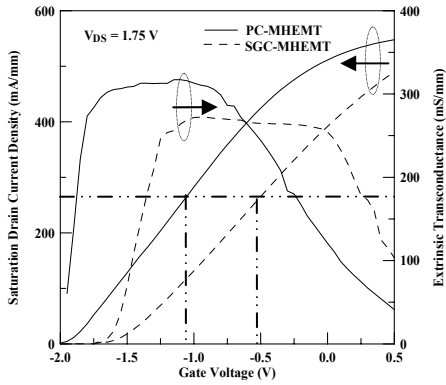


Fig. 2 g_m and I_{DSS} characteristics at $V_{DS} = 1.75$ V.

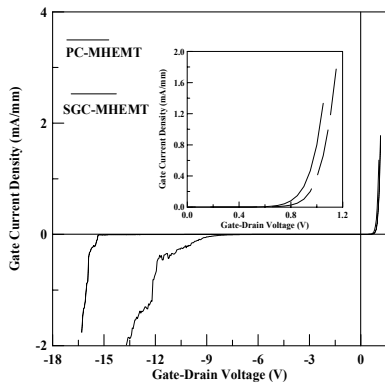


Fig. 3 Two-terminal gate-drain breakdown characteristics at 300K. The inset shows the zoomed-in forward bias characteristics.

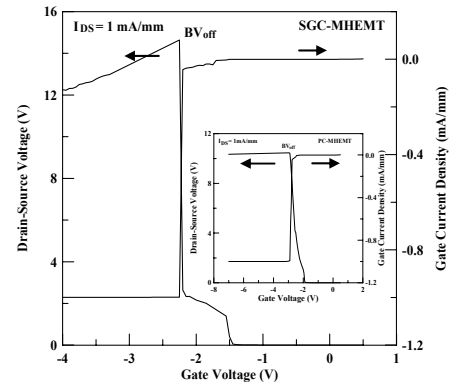


Fig. 4 Off-state breakdown characteristics of SGC-MHEMT, whereas the inset is for PC-MHEMT.

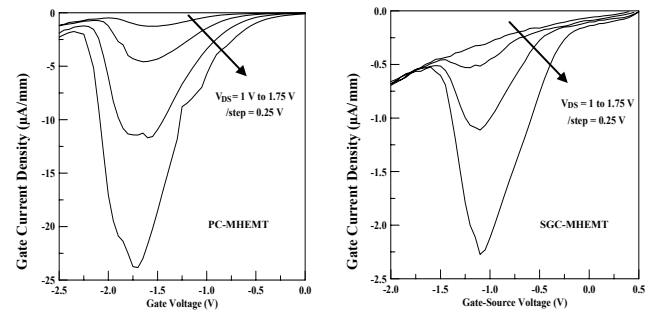


Fig. 5 On-state I_G vs. V_{GS} at various drain-source voltages.

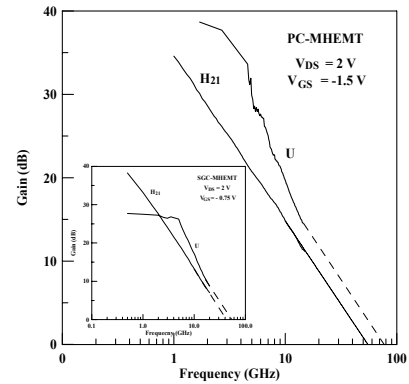


Fig. 6 Microwave characteristics, at $V_{DS} = 2$ V, for PC-MHEMT, , whereas the inset is for SGC-MHEMT.

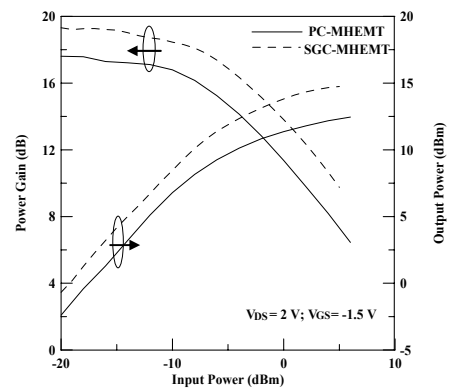


Fig. 7 Output power and power gain performances at 5.8 GHz.